Possible Explanation of the Atmospheric Kinetic and Potential Energy Spectra

Andreas Vallgren, Enrico Deusebio, and Erik Lindborg*

Linné Flow Centre, Department of Mechanics, KTH,S-100 44 Stockholm, Sweden

(Received 3 August 2011; published 20 December 2011)

We hypothesize that the observed wave number spectra of kinetic and potential energy in the atmosphere can be explained by assuming that there are two related cascade processes emanating from the same large-scale energy source, a downscale cascade of potential enstrophy, giving rise to the k^{-3} spectrum at synoptic scales and a downscale energy cascade giving rise to the $k^{-5/3}$ spectrum at mesoscales. The amount of energy which is going into the downscale energy cascade is determined by the rate of system rotation, with negligible energy going downscale in the limit of very fast rotation. We present a set of simulations of a system with strong rotation and stratification, supporting these hypotheses and showing good agreement with observations.

DOI: 10.1103/PhysRevLett.107.268501 PACS numbers: 92.60.hk, 05.45.−a

The wave number spectra of horizontal wind and temperature in the atmosphere [1–4] (Fig. 1) display a range at synoptic scales ($\sim 500 - 2000$ km) with an approximate k^{-3} dependence and a range at mesoscales ($\sim 2 - 500$ km) with a $k^{-5/3}$ dependence, where k is the horizontal wave number. The spectrum of horizontal wind can be taken to be equal to the kinetic energy spectrum while the spectrum of temperature can be translated into a potential energy spectrum, where the potential energy here is related to the restoring Archimedes force on a fluid element that is vertically displaced in a static stable atmosphere. A spectrum of the form $k^{-5/3}$ is found in 3D turbulence [5] with a downscale energy cascade, but also in 2D turbulence with an upscale energy cascade [6]. Charney [7] showed that strong rotation and stratification lead to a dynamics, which he named geostrophic turbulence, that is very similar to 2D turbulence in that there is a second quadratic invariant apart from energy. In 2D turbulence the second invariant is enstrophy (half the square of vorticity) while in geostrophic turbulence it is potential enstrophy, defined as half the square of potential vorticity, a quantity representing geostrophically balanced motions for which the velocity is tangential to the local isobar. In 2D and geostrophic turbulence enstrophy and potential enstrophy, in each case respectively, are transferred downscale which gives rise to a k^{-3} spectrum at higher wave numbers than a characteristic forcing wave number while a $k^{-5/3}$ spectrum is found at lower wave numbers.

It has been hypothesized [8–10] that the mesoscale $k^{-5/3}$ spectrum is produced by an upscale energy cascade. This hypothesis presumes that there is an important energy source at kilometer scales [11] in addition to baroclinic instability [12] at thousand kilometer scales. Apart from the difficulty in identifying the nature of this energy source, there are several other difficulties associated with this hypothesis. Since the effect of Earth's rotation is not very strong at such small scales, one has to assume that it is the effect of strong stratification that predominantly gives rise to the upscale energy cascade [9]. Numerical simulations of stratified turbulence [13–16] have shown that strong stratification alone does not favor an upscale cascade but rather a downscale cascade. Moreover, some success has been made in reproducing the transition from a k^{-3} range to a $k^{-5/3}$ range in general circulation models [17,18], mesoscale models [19,20] and idealized box simulations [21,22], without the introduction of any small-scale energy source. Despite this evidence pointing against the upscale cascade hypothesis, it was recently revived [23] on the basis of the results of an experiment in a layer of fluid with electromagnetic small-scale forcing. The authors concluded that "it is possible that the suppression of 3D

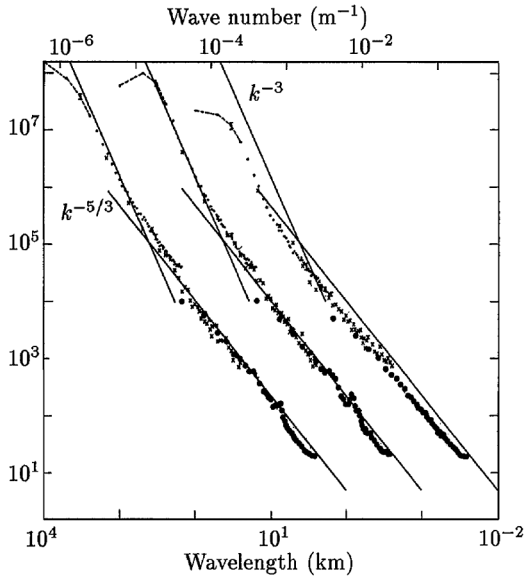

FIG. 1. Atmospheric spectra of kinetic energy of the zonal and meridional wind components and potential energy measured by means of the potential temperature. The spectra of meridional wind and potential temperature are shifted one and two decades to the right, respectively. Reproduced from Nastrom & Gage (1985).

vertical eddies induces an inverse energy cascade through the mesoscales in the Earth atmosphere.'' It is remarkable that no scientific consensus yet has been reached on the important issue whether the energy cascade through the mesoscale range is upscale or downscale.

We take a similar point of view as Tung & Orlando [24], who argued that a weak downscale energy cascade is generated from the large-scale forcing, but is shadowed by the downscale cascade of potential enstrophy, which is producing a spectrum of the form $E(k) \sim \eta^{2/3} k^{-3}$ at synoptic scales [7], where η is the flux of potential enstrophy. At a transition wave number $k_t \sim \sqrt{\eta/\epsilon}$, where ϵ is the downscale energy flux, the energy cascade will become visible and the spectrum will gradually change to $E(k) \sim \epsilon^{2/3} k^{-5/3}$. While Tung & Orlando assumed that the weak energy cascade is produced already in the limit of zero Rossby number (very strong rotation), we make the hypothesis that it is a finite Rossby number effect. To test this hypothesis, we consider the so-called primitive equations

$$\frac{D\mathbf{u}_h}{Dt} = -\nabla_h p - f\mathbf{e}_z \times \mathbf{u}_h, \tag{1a}$$

$$0 = -\frac{\partial p}{\partial z} + Nb, \tag{1b}$$

$$\frac{Db}{Dt} = -Nw, \tag{1c}$$

$$\nabla \cdot \mathbf{u} = 0, \tag{1d}$$

where $\mathbf{u}$ is the velocity vector, $\mathbf{u}_h$ is the horizontal part of $\mathbf{u}$, w is the vertical velocity component, $\mathbf{e}_z$ is the vertical unit vector, p is the pressure, N is the Brunt-Väisälä frequency, $b = g\rho/(N\rho_0)$ is the buoyancy, where ρ and ρ_0 are the fluctuating and background densities, respectively, g is the acceleration due to gravity and f is the Coriolis parameter. We reformulate the system in terms of the potential vorticity and two ageostrophic components:

$$q = -\frac{\partial u}{\partial y} + \frac{\partial v}{\partial x} + \frac{f}{N}\frac{\partial b}{\partial z}, \tag{2a}$$

$$a_1 = -\frac{f}{N}\frac{\partial v}{\partial z} + \frac{\partial b}{\partial x}, \tag{2b}$$

$$a_2 = \frac{f}{N}\frac{\partial u}{\partial z} + \frac{\partial b}{\partial y}, \tag{2c}$$

where u and v are the velocity components in the x and y direction, respectively. The equations have been subject to nondimensionalization using geostrophic scaling [7], i.e.,

$$\begin{aligned} &x \sim L, \quad y \sim L, \quad z \sim f/NL, \quad t \sim L/U, \\ &u \sim U, \quad v \sim U, \quad w \sim \mathrm{Ro}Uf/N, \quad b \sim U, \\ &q \sim U/L, \quad a_1 \sim \mathrm{Ro}U/L, \quad a_2 \sim \mathrm{Ro}U/L, \end{aligned} \tag{3}$$

where $\mathrm{Ro} = U/fL$ is the Rossby number.

Including small-scale and large-scale friction, the system can be rewritten as follows

$$\begin{aligned} \frac{\partial q}{\partial t} = &\frac{\partial}{\partial y}\left(\frac{\partial u^2}{\partial x} + \frac{\partial uv}{\partial y} + \mathrm{Ro}\frac{\partial uw}{\partial z}\right) \\ &- \frac{\partial}{\partial x}\left(\frac{\partial uv}{\partial x} + \frac{\partial v^2}{\partial y} + \mathrm{Ro}\frac{\partial vw}{\partial z}\right) \\ &- \frac{\partial}{\partial z}\left(\frac{\partial ub}{\partial x} + \frac{\partial vb}{\partial y} + \mathrm{Ro}\frac{\partial wb}{\partial z}\right) \\ &+ \nu_S \nabla^8 q - \nu_L q, \end{aligned} \tag{4a}$$

$$\begin{aligned} \mathrm{Ro}\frac{\partial a_1}{\partial t} = &a_2 - \frac{\partial w}{\partial x} + \frac{\partial}{\partial z}\left(\frac{\partial uv}{\partial x} + \frac{\partial v^2}{\partial y} + \mathrm{Ro}\frac{\partial vw}{\partial z}\right) \\ &- \frac{\partial}{\partial x}\left(\frac{\partial ub}{\partial x} + \frac{\partial vb}{\partial y} + \mathrm{Ro}\frac{\partial wb}{\partial z}\right) \\ &+ \mathrm{Ro}\nu_S \nabla^8 a_1 - \mathrm{Ro}\nu_L a_1, \end{aligned} \tag{4b}$$

$$\begin{aligned} \mathrm{Ro}\frac{\partial a_2}{\partial t} = &-a_1 - \frac{\partial w}{\partial y} - \frac{\partial}{\partial z}\left(\frac{\partial u^2}{\partial x} + \frac{\partial uv}{\partial y} + \mathrm{Ro}\frac{\partial uw}{\partial z}\right) \\ &- \frac{\partial}{\partial y}\left(\frac{\partial ub}{\partial x} + \frac{\partial vb}{\partial y} + \mathrm{Ro}\frac{\partial wb}{\partial z}\right) \\ &+ \mathrm{Ro}\nu_S \nabla^8 a_2 - \mathrm{Ro}\nu_L a_2. \end{aligned} \tag{4c}$$

$$0 = \frac{\partial u}{\partial x} + \frac{\partial v}{\partial y} + \mathrm{Ro}\frac{\partial w}{\partial z} \tag{4d}$$

Apart from the viscous parameters, the Rossby number constitutes the single adjustable parameter that enters the equations, whereas the Froude number, $\mathrm{Fr} = U/LN$, is implicitly set to zero through the assumption (1b) of hydrostatic balance [25]. The inviscid, unforced system conserves total energy, $(u^2 + v^2 + b^2)/2$. In the limit $\mathrm{Ro} = 0$, it reduces to Charney's equation [7] which apart from energy also conserves potential enstrophy, $q^2/2$.

The system (4) is solved using a pseudo spectral method, with full dealiasing, in a triply-periodic $(2\pi \times 2\pi \times 2\pi)$ domain with a resolution of 1024^3 grid points. Observe that the box is cubic in the space where the vertical coordinate is stretched by a factor of N/f. Translated to midlatitude atmospheric dynamics this would correspond to a real space box aspect ratio of $f/N \sim 0.01$. The velocities and the buoyancy are recovered by inverting the nondimensional counterpart of (2) which contains the Rossby number but not the Froude number. A random forcing is introduced in the potential vorticity equation. The forcing is white noise in time and restricted to the wave number shell $k \in [3,5]$, i.e., it is isotropic in the space where the vertical coordinate has been stretched. The potential enstrophy injection rate, η, is perfectly controlled and is set to unity. Consequently, the energy injection rate, P, is also a controlled parameter. We carry out six simulations for $\mathrm{Ro} = [0, 0.025, 0.05, 0.075, 0.1, 0.2]$ and the corresponding values $\nu_S = [2.4, 1.9, 1.9, 1.9, 4.0, 6.2] \times 10^{-18}$ of the small-scale viscous parameter, while the large-scale viscous parameter has the same value $\nu_L = 0.12$ in all simulations. The Rossby number can also be interpreted as

$\mathrm{Ro} = \eta^{1/3}/f$. Cho and Lindborg [26] made the estimate $\eta \sim 10^{-15}$ s^{-3} from structure function analyses in lower stratosphere. If this value is representative for the atmosphere we would obtain $\mathrm{Ro} \sim 0.1$ at midlatitude. The reason why we have increased ν_S in the two highest Rossby number simulations is that a larger amount of energy is going downscale in these simulations. To make sure that dissipation takes place at the resolution scale, Δx, we need a ν_S scaling as $\sim \epsilon^{1/3}(\Delta x)^{22/3}$, where ϵ is the downscale energy flux.

The total spectral energy flux can be calculated as

$$\Pi(k) = -\sum_{k'=0}^{k} \mathrm{Im}[k_x(\hat{u}^2\hat{u}^* + \widehat{u\upsilon}\hat{\upsilon}^* + \widehat{ub}\hat{b}^*) + k_y(\hat{\upsilon}^2\hat{\upsilon}^* + \widehat{u\upsilon}\hat{u}^* + \widehat{\upsilon b}\hat{b}^*) + \mathrm{Ro}k_z(\widehat{uw}\hat{u}^* + \widehat{\upsilon w}\hat{\upsilon}^* + \widehat{wb}\hat{b}^*)], \quad (5)$$

where the hat denotes the Fourier transform and $k' = \sqrt{k_x^2 + k_y^2 + k_z^2}$. In Fig. 2(a), we see $\Pi(k)$ normalized by the energy injection rate P. There is a monotonic decrease of Π/P with increased rate of rotation. For all Rossby numbers, there is a range of constant positive flux, ϵ, showing that there is a downscale energy cascade. In each constant energy flux range there is negligible dissipation. For $\mathrm{Ro} = 0$ less than 1000th of the injected energy is going downscale. For $\mathrm{Ro} > 0$, we find that $\epsilon \propto \mathrm{Ro}^{1.5}P$, approximately. In Fig. 2(b), we see the horizontal spectra of total energy. For both $\mathrm{Ro} = 0.2$ and $\mathrm{Ro} = 0.1$ we find a clear range where the total energy spectrum scales as $E(k) = C\epsilon^{2/3}k^{-5/3}$, with $C \approx 1.1$ for $\mathrm{Ro} = 0.2$ and $C \approx 1.4$ for $\mathrm{Ro} = 0.1$. We find that the ratio between the kinetic and potential energy is a little bit larger than 2 in this range, consistent with previous simulations of stratified turbulence [14]. For $\mathrm{Ro} = 0$, the spectrum is slightly steeper than, but close to, $\mathcal{K}\eta^{2/3}k^{-3}$ with $\mathcal{K} \approx 2.2$, consistent with the prediction of Charney [7] and previous simulations of geostrophic turbulence [27]. For $\mathrm{Ro} = 0.025$, the spectrum is slightly more shallow than k^{-3}.

The sign and the magnitude of the kinetic energy flux, ϵ_K, can be estimated by measuring third-order velocity structure functions, which are third-order statistical moments of differences between the velocity components measured at two points which are separated by a distance r. Kolmogorov [28] derived the relation $D_{LLL} = -4\epsilon_K r/5$, for the longitudinal third-order structure function of isotropic 3D turbulence, where L refers to the direction of the separation vector $\mathbf{r}$. For 2D turbulence a similar derivation [29] gives $D_{LLL} = -3\epsilon_K r/2$ where ϵ_K in this case is negative since the cascade is upscale. In the enstrophy cascade range of 2D turbulence one finds that $D_{LLL} = \eta r^3/8$, where η here is the enstrophy flux [29]. Wind data from the lower stratosphere were used [26] to calculate the sum $D = D_{LLL} + D_{LTT}$, where T refers to a velocity component perpendicular to $\mathbf{r}$. It was found that D has a negative linear dependence on r at mesoscales. At $r \approx 300$ km, D switches sign and at synoptic scales there is a narrow range where D approximately scales as $\sim r^3$. In Fig. 3(a) we see that D is preferentially negative in the higher Rossby number runs, with a change of sign moving towards larger scales with increasing Rossby number. In the highest Rossby number runs we find that $D \approx -2\epsilon_K r$, in the forward energy cascade range, which is the relation that was used [26] to estimate ϵ_K. In Fig. 3(b) we see that D is preferentially positive for the lowest Rossby number runs for which $D \sim r^3$, with a particular good agreement for $\mathrm{Ro} = 0$.

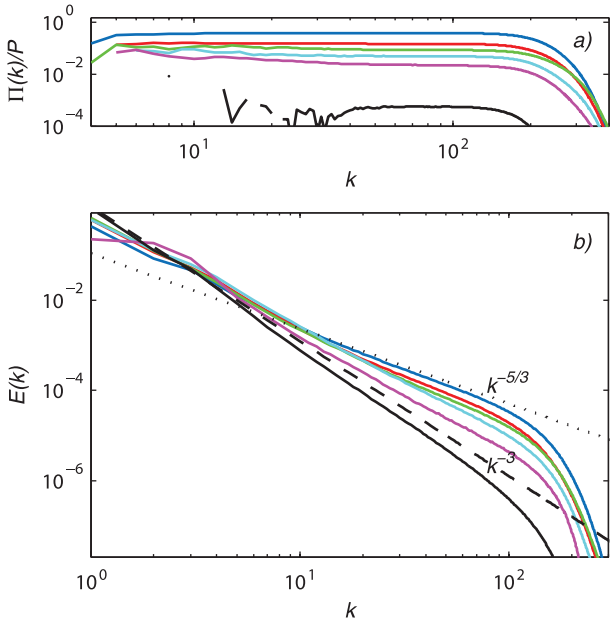

FIG. 2 (color). (a) Energy flux as a function of wave number k normalized by the energy injection rate. The magnitude of the flux is increasing with increasing Rossby number. From bottom to top: $\mathrm{Ro} = [0, 0.025, 0.05, 0.075, 0.1, 0.2]$, (b) energy spectrum for different Rossby numbers with the same colors as in (a). The k^{-3} (dashed) and $k^{-5/3}$ slopes (dotted) are indicated.

With a forcing acting at a particular wave number k_f the enstrophy and the energy injection rates are approximately related as $\eta = k_f^2 P$. With $\epsilon \sim \mathrm{Ro}^{3/2}P$ we can thus estimate the transition wave number as $k_t \sim \sqrt{\eta/\epsilon} \sim \mathrm{Ro}^{-3/4}k_f$. In the atmosphere, the most unstable wave number of baroclinic instability can be estimated as $k_f \sim 2\pi/(4L_R)$, where L_R is the Rossby deformation radius. If the relation $\epsilon \sim \mathrm{Ro}^{3/2}P$ also would hold in the atmosphere, we would thus obtain a transition wave number $k_t \sim \pi\mathrm{Ro}^{-3/4}/(2L_R)$ and a corresponding transition scale $L_t \sim 4L_R\mathrm{Ro}^{3/4}$. With $L_R = 1000$ km and $\mathrm{Ro} = 0.1$, we obtain $L_t \sim 700$ km, in reasonable agreement with observations (Fig. 1).

In agreement with previous simulations [18,20,22,30] and data analysis [31], our simulations show that the kinetic energy content in horizontally divergent modes is

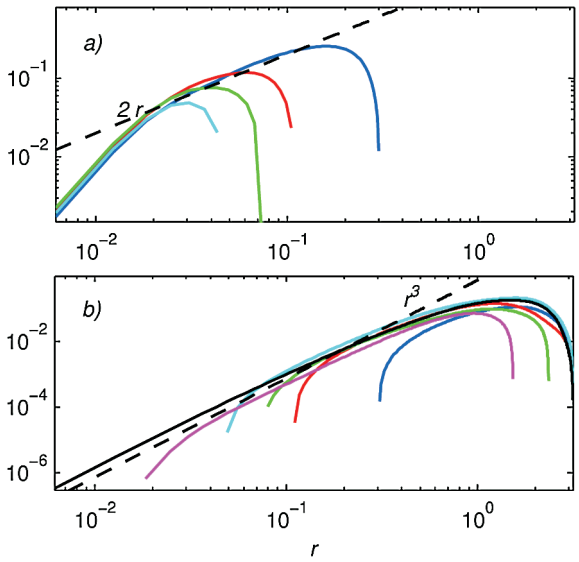

FIG. 3 (color). Third-order structure function D, for different Rossby numbers, with the same colors as in Fig. 2. (a) Negative range normalized by the kinetic energy dissipation rate, (b) positive range normalized by the enstrophy injection rate. The theoretically predicted slopes are indicated.

of the same order of magnitude as the content in rotational modes, in the mesoscale range. Koshyk and Hamilton [30] interpreted the energy content in the divergent modes as a signal of gravity waves. In a future study, we will address the issue of the possible importance of gravity waves by carrying out frequency analyses.

In conclusion, our numerical experiment shows that the same type of spectrum as found in the atmosphere can be generated from a single energy source in a system with strong stratification and strong but finite rotation. The experiment suggests that the atmospheric $k^{-5/3}$ mesoscale spectrum can be explained by the existence of a downscale energy cascade whose strength is regulated by the Rossby number. Moreover, the simulations show a third-order structure function, D, which is consistent with observations from the lower stratosphere.

Computer time provided by SNIC (Swedish National Infrastructure for Computing) is gratefully acknowledged.

*erikl@mech.kth.se

[1] G. D. Nastrom, K. S. Gage, and W. H. Jasperson, Nature (London) **310**, 36 (1984).
[2] G. D. Nastrom and K. S. Gage, J. Atmos. Sci. **42**, 950 (1985).
[3] J. Y. N. Cho, R. E. Newell, and J. D. Barrick, J. Geophys. Res. **104**, 16 297 (1999).
[4] R. Frehlich and R. Sharman, J. Appl. Meteor. Climatol. **49**, 1149 (2010).
[5] A. N. Kolmogorov, Dokl. Akad. Nauk SSSR **30**, 301 (1941).
[6] R. H. Kraichnan, Phys. Fluids **10**, 1417 (1967).
[7] J. G. Charney, J. Atmos. Sci. **28**, 1087 (1971).
[8] K. S. Gage, J. Atmos. Sci. **36**, 1950 (1979).
[9] D. K. Lilly, J. Atmos. Sci. **40**, 749 (1983).
[10] G. Falkovich, Phys. Rev. Lett. **69**, 3173 (1992).
[11] D. K. Lilly, J. Atmos. Sci. **46**, 2026 (1989).
[12] G. K. Vallis, *Atmospheric and Oceanic Fluid Dynamics: Fundamentals and Large-scale Circulation; Electronic Version* (Cambridge University Press, Leiden, 2006).
[13] J. J. Riley and S. M. deBruynKops, Phys. Fluids **15**, 2047 (2003).
[14] E. Lindborg, J. Fluid Mech. **550**, 207 (2006).
[15] G. Brethouwer, P. Billant, E. Lindborg, and J.-M. Chomaz, J. Fluid Mech. **585**, 343 (2007).
[16] J. P. Laval, J. C. McWilliams, and B. Dubrulle, Phys. Rev. E **68**, 036308 (2003).
[17] Y. O. Takahashi, K. Hamilton, and W. Ohfuchi, Geophys. Res. Lett. **33**, L12 812 (2006).
[18] K. Hamilton, Y. O. Takahashi, and W. Ohfuchi, J. Geophys. Res. **113**, D18 110 (2008).
[19] W. C. Skamarock, Mon. Weather Rev. **132**, 3019 (2004).
[20] W. C. Skamarock and J. B. Klemp, J. Comput. Phys. **227**, 3465 (2008).
[21] Y. Kitamura and Y. Matsuda, Geophys. Res. Lett. **33**, L05809 (2006).
[22] M. J. Molemaker and J. C. McWilliams, J. Fluid Mech. **645**, 295 (2010).
[23] H. Xia, D. Byrne, G. Falkovich, and M. Shats, Nature Phys. **7**, 321 (2011).
[24] K. K. Tung and W. W. Orlando, J. Atmos. Sci. **60**, 824 (2003).
[25] P. Billant and J.-M. Chomaz, Phys. Fluids **13**, 1645 (2001).
[26] J. Y. N. Cho and E. Lindborg, J. Geophys. Res. **106**, 10 223 (2001).
[27] A. Vallgren and E. Lindborg, J. Fluid Mech. **656**, 448 (2010).
[28] A. N. Kolmogorov, Dokl. Akad. Nauk SSSR **32**, 16 (1941).
[29] E. Lindborg, J. Fluid Mech. **388**, 259 (1999).
[30] J. N. Koshyk and K. Hamilton, J. Atmos. Sci. **58**, 329 (2001).
[31] E. Lindborg, J. Atmos. Sci. **64**, 1017 (2007).